

# ATTITUDE CHARACTERIZATION OF AERODYNAMIC STABLE OBJECTS BASED ON TLE

C. Parigini<sup>(1)</sup>, D. Bonetti<sup>(1)</sup>, Gonzalo Blanco Arnao<sup>(1)</sup>, N. Sanchez-Ortiz<sup>(1)</sup>, S. Lemmens<sup>(2)</sup>

<sup>(1)</sup> Deimos Space, Tres Cantos, Madrid, 28760, Spain, Email: {cristina.parigini, davide.bonetti, gonzalo.blanco, noelia.sanchez} @ deimos-space.com

<sup>(2)</sup> ESA/ESOC Space Debris Office (OPS-GR), Robert-Bosch-Str. 5, 64293 Darmstadt, Germany, Email: Stijn.Lemmens@esa.int

## ABSTRACT

The problem of reconstructing the body attitude from TLE is difficult due to the accuracy of TLE information and data frequency. However, attitude could be reconstructed when additional information is available, for instance, optical measurements or when additional assumptions could be made (e.g. stable attitude behavior).

In this paper we present the main outcomes of the work performed within the *Bench-marking Reentry Predictions* ESA study, where we analyzed space objects that present similarities with GOCE in terms of aerodynamic stability and geometry.

## 1 INTRODUCTION

In re-entry predictions, drag plays a critical role as it is the main force driving the orbital decay in Low Earth Orbits: according to [1], it is the most significant orbit perturbation that affects the semi-major axis in a secular manner. Other perturbations affect the semi-major axis, but most average out over an orbit cycle due to their periodic character. Some perturbations, however, do cause a secular variation in the semi-major axis, such as the combination of solar radiation pressure and gravity anomalies as a satellite passes in and out of Earth's shadow. However, these variations are small compared to those produced by drag, and they are neglected in this work.

Estimation of the drag is not easy due to the large uncertainties on the atmospheric properties and drag area. Focusing on the latter, attitude knowledge is critical: it has a direct impact not only on the drag coefficient but also on the effective area where the aerodynamic perturbations are exerting the force. Therefore, attitude knowledge reduces the uncertainty on the estimation of drag which means an improvement in the re-entry time estimation.

The problem of reconstructing the body attitude from TLE is difficult due to the accuracy of TLE information and data availability frequency: only rough estimations of the BC could be obtained from TLE and with this

information it is not possible to reconstruct accurately the attitude. However, attitude could be reconstructed when additional information is available, for instance, when optical measurements are available [2] or when additional assumptions could be made (e.g. stable attitude behavior). In this frame, GOCE attitude behavior presents the ideal case where very small variability in the yaw and pitch angles is observed in the last weeks before entry.

In this paper we present the main outcomes of the work done within the *Bench-marking Reentry Predictions* ESA study, led by Deimos Space, where we analyzed space objects that present similarities with GOCE in terms of aerodynamic stability and geometry (e.g. elongated bodies). A preliminary analysis of the critical parameters and ranges that guarantee a stable flight at high altitude is done based on Flying Quality analysis for simple shape objects (e.g. cylinder and box). These results are then used as a filter applied to DISCOS database to select 5 objects among the known debris including both rocket bodies and payloads that re-entered in the past. For such objects, 3-DoF and 6-DoF simulations and TLE analysis are combined to characterize the attitude during the orbital decay. GOCE is used to benchmark the approach followed.

## 2 APPROACH

A schematic overview of the approach followed is shown in Fig. 1. The work has been split in two main parts:

- Object analysis and selection, presented in section 3.
- Object trajectory simulation, presented in section 4

Concerning the object analysis and selection, the idea is to identify first the conditions under which a stable flight is possible, based on the analysis of the aerodynamics of simple geometric shapes. Once the ranges of feasible conditions for a stable flight are determined, objects compatible with these conditions are searched, also fulfilling other additional criteria (e.g. circular orbit, elongated body). Finally, among the

resulting subset of rocket bodies and payloads, five interesting candidates are selected for the accurate estimation of their ballistic coefficients ( $BC = m/SC_D$ ).

For the selected objects a wide set of trajectory simulation and analysis have been performed, based on:

- 6-DoF simulations on a reduced number of orbits, for verification of the validity of stable motion and attitude laws assumption.
- 3-DoF simulations on an extended number of orbits based on given attitude profiles (under the assumption of stable flight conditions, verified with 6-DoF runs).
- Analysis of TLE covering the full range of epochs available, including atmospheric uncertainties.

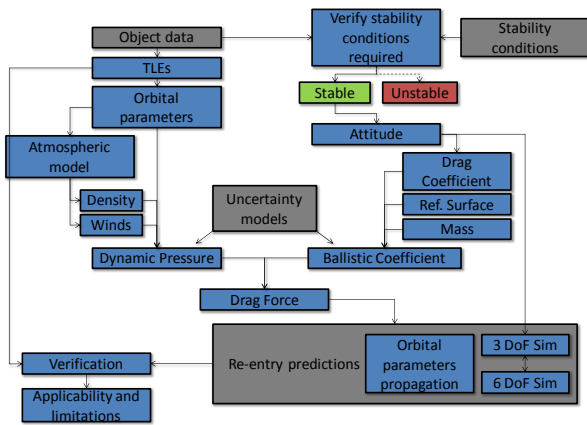


Figure 1 Schematization of the approach followed

The analyses are based on the Planetary Entry Toolbox [3] which is a Software suite developed by Deimos Space S.L.U. to support Mission Engineering and Flight Mechanics in the area of Atmospheric Flight. In particular, the following modules have been used:

- 3DoF/6DoF high fidelity propagation (EndoSim module) in open loop
- Aerodynamic analysis module: inspection and generation (HYDRA).
- Flying Qualities Analysis Tool [4]

Additionally, the ESA DISCOS database has been used to identify the interesting debris [5].

### 3 OBJECT ANALYSIS AND SELECTION

The Object analysis has been based on the analysis of the Flying Quality (FQ). Focus is done on the aerodynamic static stability at high altitudes for simple geometric shapes (box and cylinder) with variable size, together with GOCE as a reference case. Both Continuum (cont) and Free Molecular Flow (FMF) aerodynamics (force and moment coefficients) have been computed based on local inclination methods (HYDRA tool). A bridging function is applied to

estimate the aerodynamics properties in rarefied regime. Concerning the FQ, the following parameters are estimated:

- **Trim attitude:** it is the equilibrium point where the aerodynamic moments are zero. Trim angles depend on the aerodynamic shape and on the position of the centre of gravity: given the symmetry of the shapes considered, only half domain (moving CoG from nose to 50% of the reference length) in the symmetry plane ( $X-Z$ ,  $Y=0$ ) has been studied.
- **Longitudinal static stability** behaviour around the trim condition has been analysed based on the aerodynamic stability derivative ( $Cm_\alpha$ ) and on the longitudinal static margin ( $SM$ ), which is a measure of the distance between the centre of gravity and the neutral point (point at which stability is neutral).
- **Lateral-Directional static stability** behaviour around the trim condition has been analysed based on the aerodynamic stability derivatives ( $Cn_\beta$ ,  $Cl_\beta$ ) and on the dynamic  $Cn_\beta$  which is a generalization of the classical criterion based on  $Cn_\beta$ , valid also in case of flight at high angles of attack.

The maps for the **cylindrical shape** for both continuum and FMF regimes, in terms of trim angle of attack, longitudinal static margin and dynamic  $Cn_\beta$ , are shown respectively in Fig. 2, Fig. 3 and Fig. 4. The effect of changing the dimensions ratio ( $L/D = \text{Length/Diameter}$ ), from short to elongated shape, can be seen moving from the left to the right plot. For the same CoG location (relative to the dimension of the specific object under analysis), higher trim angles corresponds to shorter shapes. Lower values are obtained in continuum regime. Concerning the static margin, the driver here is the longitudinal position of the centre of gravity: forward CoG locations are better. Finally, lateral-directional static stability is found in almost all the domain but degradation of the stability is expected moving from FMF to continuum regime and for elongated shapes.

No significant differences have been observed between the cylinder and the box results. Instead, differences above 30% in the lateral-directional parameters are obtained in case of GOCE shape: this is due to its lateral panels which significantly affect its stability.

It is also important to remind that due to the symmetry of these shapes, two trim conditions are found for each CoG position: one corresponds to a statically stable condition (trim AoA shown here) and one to an unstable condition (trim AoA+180°).

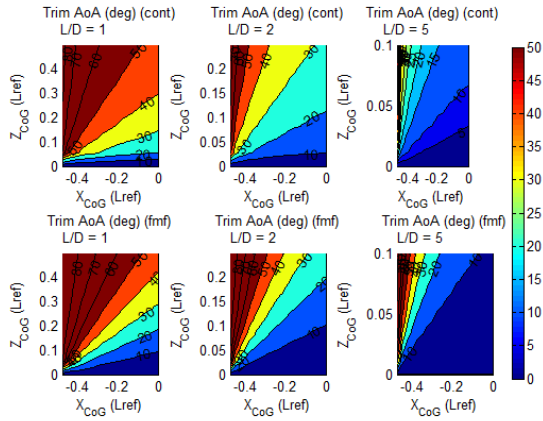


Figure 2 Trim angle of attack for a cylinder characterized by  $L/D = 1, 2$  and  $5$  (from left to right) in Continuum and Free Molecular Flow (top and bottom)

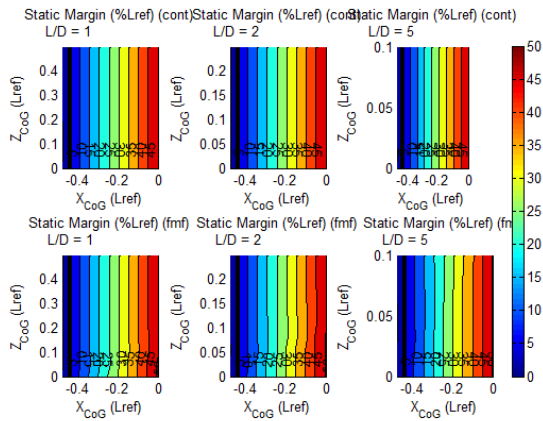


Figure 3 Longitudinal static margin for a cylinder characterized by  $L/D = 1, 2$  and  $5$  (from left to right) in Continuum and Free Molecular Flow (top and bottom)

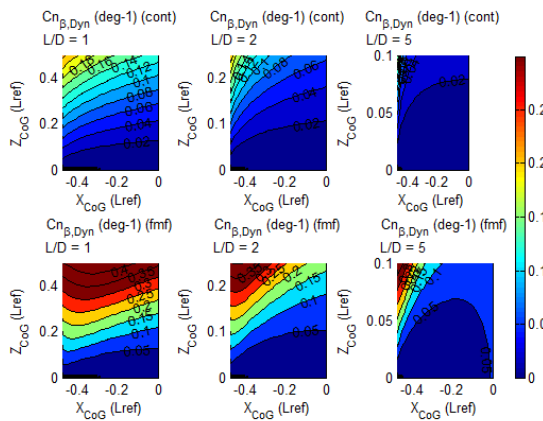


Figure 4 dynamic  $Cn_{\beta}$  for a cylinder characterized by  $L/D = 1, 2$  and  $5$  (from left to right) in Continuum and Free Molecular Flow (top and bottom)

Globally, boxes and cylinders with dimension ratio between 2 and 5 guarantee on one side good stability properties in almost the whole CoG domain and for the other sufficient variability in the drag coefficient depending on the attitude flown. As an example, the drag coefficient map depending on the attitude for an elongated box ( $L/H = 3$ ) is presented in Fi5.

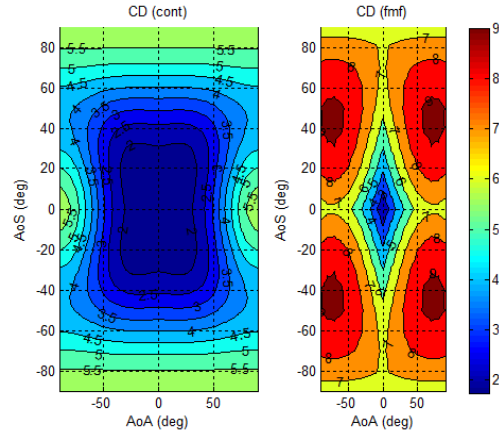


Figure 5 Drag coefficient map in Continuum (left) and Free Molecular Flow (right) for a box characterized by  $L/H = 3$

Following FQ analyses, a subset of space objects have been identified as a result of DISCOS database filtering process based on the following criteria:

- Known objects: this is necessary to have information about the actual shape and mass.
- Primary shapes: box and cylinder characterized by a dimension ratio between 3 and 6. Concerning the dimension ratio, this range is slightly shifted to higher values as the filter has been applied before the final consolidation of FQ results presented here.
- Circular orbit (eccentricity  $< 0.001$ ), to select objects in orbital condition similar to GOCE.
- Re-entry epoch after 1995 to improve the TLE quality available.

This filtering criteria result in 17 space objects, listed in Table 1, which are classified as follow:

- 10 rocket bodies and in particular upper stages (light blue), and 7 payloads (orange).
- 10 cylinders (green), 4 box (yellow) and 3 more complex shapes. Cylindrical objects correspond to the upper stages.

The five candidates selected are highlighted in bold: among the upper stages, the objects with higher  $L/D$  have been chosen; concerning the payloads, two 3-unit cubeSats have been selected. The estimated variability of the ballistic coefficient based on FMF aerodynamics for these objects is presented in Fig. 6, where GOCE values are also reported for comparison purposes; blue

and green points correspond respectively to the upper stages and payloads. Five values are shown for each object:

- Minimum and maximum BC: the global variability depending on the attitude results to be wide, being the maximum value 4-5 times the minimum one. GOCE shape results in an even higher variability.
- BC corresponding to the trim attitude: assuming a CoG located along the symmetry axis, this value is the same as the maximum BC, which corresponds to the minimum drag.
- An average value for  $\pm 5^\circ$  attitude oscillation around the trim. This leads to estimations a bit lower than the maximum values, between -20% and -30%.
- In case of a random tumbling motion, the BC is close to the minimum BC.

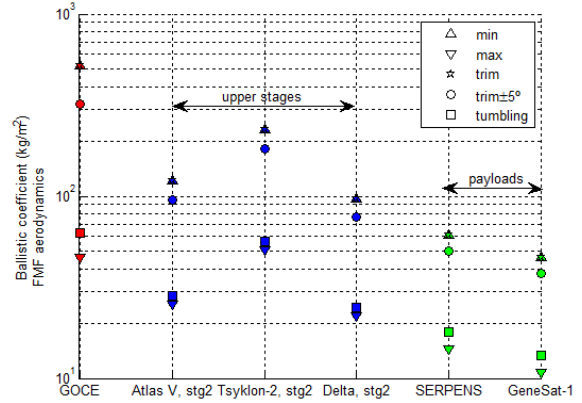


Figure 6 Ballistic coefficient variability depending on attitude

Table 1 Filtered objects, selected ones in bold

SatNo	Name	Shape	Length (m)	Height (m)	Depth (m)	Re-entry Epoch
388	Scout X-2M stage 4 (M-2)	Cylinder	0.46	1.50	1.50	03-may-99
229	Delta stage 3 (X-248)	Cylinder	0.46	1.50	1.50	10-aug-02
165	Delta stage 3 (X-248)	Cylinder	0.46	1.50	1.50	19-feb-14
<b>3019</b>	<b>Tsyklon-2 stage 2</b>	<b>Cylinder</b>	<b>3.00</b>	<b>10.89</b>	<b>10.89</b>	<b>27-dec-02</b>
21148	Titan IVA stage 2	Cylinder	3.05	9.96	9.96	09-jan-99
<b>6895</b>	<b>Delta 1604 stage 2 (AJ10-118F)</b>	<b>Cylinder</b>	<b>1.43</b>	<b>4.90</b>	<b>4.90</b>	<b>29-nov-96</b>
22013	Scout G-1 stage 4 (Altair IIIA)	Cylinder	0.46	1.50	1.50	28-jan-02
24745	Start-1 stage 5	Cylinder	1.50	0.50	1.50	12-jan-01
23857	SAX	Cylinder + wings	2.72	3.62	14.20	29-apr-03
23858	Atlas I second stage (Centaur I)	Cylinder	3.10	10.10	10.10	09-jun-00
28098	Gruzomaket	Cyl + Box	0.80	2.50	2.5	15-dec-15
<b>29655</b>	<b>Genesat-1</b>	<b>Box</b>	<b>0.10</b>	<b>0.30</b>	<b>0.30</b>	<b>04-aug-10</b>
<b>30778</b>	<b>Atlas V second stage (Centaur)</b>	<b>Cylinder</b>	<b>3.10</b>	<b>11.70</b>	<b>11.70</b>	<b>22-dec-14</b>
40456	GEARRS	Box	0.10	0.30	0.30	07-nov-15
40280	RK-21-8	Box + 1 Ant	1.20	0.50	1.90	11-mar-15
40457	MicroMAS	Box	0.10	0.30	0.30	01-aug-15
<b>40897</b>	<b>SERPENS</b>	<b>Box</b>	<b>0.10</b>	<b>0.30</b>	<b>0.30</b>	<b>27-mar-16</b>

## 4 OBJECT TRAJECTORY SIMULATION

### 4.1 6-DoF and 3-DoF Simulation

A wide set of 6-DoF (open-loop) and 3-DoF simulations is run to verify the aerodynamic stability of the object under analysis and to check the consistency of the

attitude performance models.

Initial conditions come from TLE and two sets of initial attitude and rates have been tested: trim attitude and null rates;  $\pm 10^\circ$  error on trim AoA and AoS and non-null initial rates ( $\pm 0.1$  deg/s). Trajectory duration is 5 h, which corresponds to 3-4 revolutions in case of 6-DoF simulation and 3 days in 3-DoF.

MCI properties are estimated based on the available information of dimensions and mass: simplified assumptions are made for the rocket bodies (modelled as a point mass engine plus a cylindrical shell for the tank), while just a guess is used for the payload. This means that even if the attitude stability characterization remains applicable, the real attitude oscillations cannot be estimated.

The atmospheric model is NRLMSISE-00 which depends on position (altitude, latitude and longitude) and epoch. Solar flux parameters are also varied based on epoch. No winds are modelled. Gravity model is based on EGM96 and 4 harmonics are considered. No other trajectory or attitude perturbations are included in the simulation to focus the analysis on the aerodynamics effects. From the trajectory point of view only short simulations are run so the impact of perturbation such as third body, solar radiation pressure is minor. Concerning the attitude perturbations, the order of magnitude of the gravity gradient and the solar radiation pressure perturbations is compared to that of the aerodynamic perturbation in Fig. 7: below 300 km the impact of the aerodynamics becomes dominant so, for the objects under considerations, below such altitude the attitude dynamics is driven by aerodynamics.

The impact of the initial altitude is shown in Fig. 8 for the Tsyklon second stage. The importance of the aerodynamic torque perturbation is strongly dependent on the dynamic pressure and therefore on the altitude. Higher is the aerodynamic torque and higher is the restoration moment produced that tends to stabilize the

object (a statically stable trim condition is selected here). Three regimes are identified based on a qualitative analysis of all the 6-DoF simulation results (graphically shown the shading colour red/yellow/green): above 450 km the attitude motion is driven by the inertial dynamics; between 450 km and 250 km attitude dynamics depends on both inertial motion and aerodynamics and the impact of the aerodynamics depends on several factors, as the MCI properties and initial conditions; below 250 km the attitude motion is driven by the aerodynamics where the aerodynamic stability condition is verified.

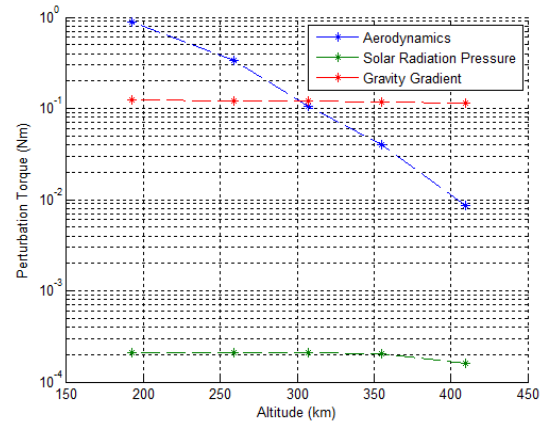


Figure 7 Attitude perturbations magnitude as function of altitude, ATLAS V second stage

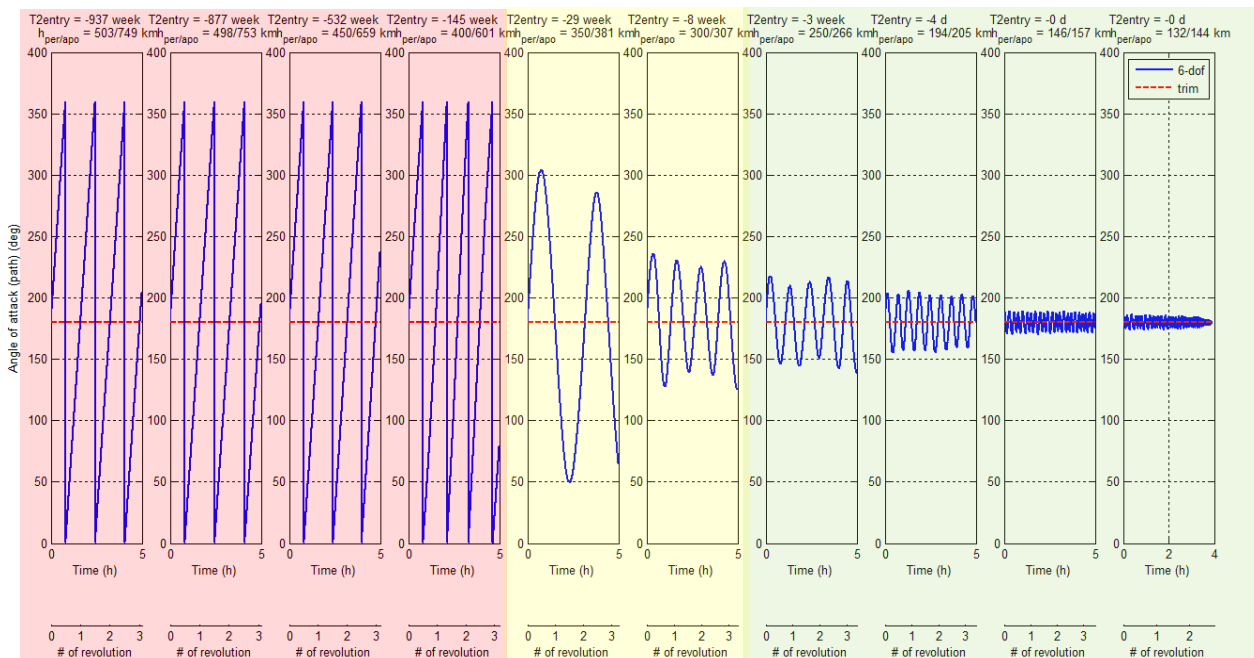


Figure 8 Tsyklon second stage for different initial pericentre altitude from 500 km down to 132 km (left to right plot), initial trim attitude and null rates

Concerning the 3-DoF simulations, results have been analyzed to check the consistency with 6-DoF simulations in terms of pericentre and apocentre decay.

The results for Delta second stage (250 km pericentre), are shown in Fig. 9: the  $\pm 30^\circ$  attitude performance model is quite well representative of the 6-DoF simulations; however the error with respect to TLE, shown in Fig. 10, suggests that the real oscillation amplitude is around  $\pm 5^\circ$ . Similar results are obtained also in another rocket body (Tskylon) and one payload (GeneSat-1): in these cases the 6-DoF simulation seems to respectively underestimate and overestimate the real oscillations amplitude. The inconsistency between the 6-DoF simulations and TLE in these three cases is probably due to a wrong estimation of the MCI properties which strongly affect the oscillation amplitude. Concerning the Atlas V second stage the  $\pm 30^\circ$  attitude performance model is quite well representative of the 6-DoF simulations, however it slightly underestimate the real amplitude oscillations which are expected to be a bit higher, as demonstrated in the next section. Finally, a totally unexpected behaviour results for the SERPENS payload. In this case there is no attitude performance mode in agreement with TLE. A possibility is that this spacecraft is not performing an uncontrolled entry. Another possible explanation is that the data about the vehicle in terms of mass, shape and size is not correct.

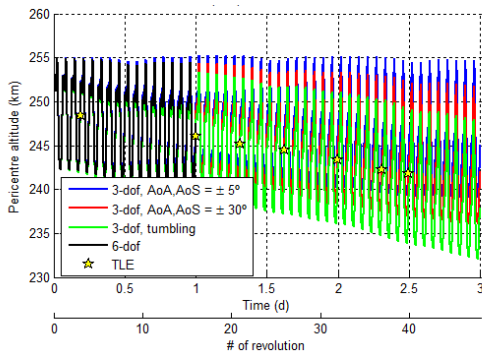


Figure 9 Apocentre altitude, Delta second stage, initial conditions at 250 km pericentre

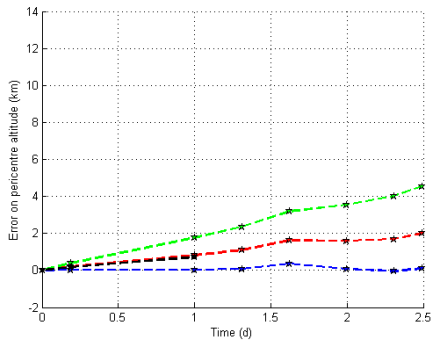


Figure 10 Apocentre altitude error with respect to TLE, Delta second stage

## 4.2 Analysis of TLE

The main objective of the TLE analysis is the estimation of the ballistic coefficient in the whole range of epoch where TLE are available. This allows us to compare this estimation with the expected BC variability. Additionally an attitude performance model is proposed, together with the verification of the aerodynamic stable attitude motion assumption. Focus is set on the results for altitude below 300 km as above such altitudes aerodynamics is not the driver of the attitude motion. The following assumptions are made:

- The drag acceleration is computed based on the semi-major axis derivative considering only drag losses, as the other perturbations are averaged over an orbit cycle. Also, no filtering is applied on TLE data.
- The BC is estimated considering the NRLMSISE-00 atmospheric density and a solar activity modelled depending on epoch. Additionally, a  $\pm 3\sigma$  band on density derived from GOCE data is also applied. It is clear that this variability is not applicable outside the GOCE altitude and epoch range; in any case it gives an indication of the potential variability due to atmosphere uncertainty.

GOCE results, shown in Fig. 11 have been used to benchmark this approach, as the real attitude is known. In this case, the ballistic coefficient estimated is inside the expected variability in the whole range of data available (3 weeks before entry). Only few points are extremely outside the range: filtering TLE should avoid this issue. As expected, the results are globally consistent with attitude oscillations of  $\pm 5^\circ$  until the last few days where a slight lowering of the BC is noted (related to an increasing of the attitude oscillations).

The results for the Tsyklon second stage are shown in Fig. 12. Results are shown for altitudes below 300 km, corresponding to the last 8 weeks before entry. In this range, the ballistic coefficient is compatible with a stabilized attitude with oscillations around  $10^\circ$  until the last week before entry. At this point the oscillations seem to grow up to  $25^\circ$ . Similar behaviour, with different oscillation amplitudes, is obtained for the GeneSat-1 payload and Delta second stage, shown respectively in Fig. 14 and Fig. 15. In GeneSat-1, the motion seems to turn into a tumbling motion 1 week before entry. Concerning the Atlas V second stage, shown in Fig. 13, the ballistic coefficient is compatible with both a tumbling motion and a stabilized attitude with large oscillations (between  $40^\circ$  and  $60^\circ$ ). Results for the SERPENS payload are not shown, but again, the BC is totally outside the expected variability.

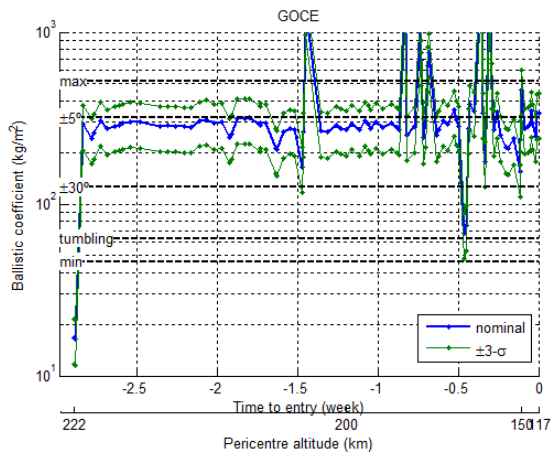


Figure 11 BC estimation, GOCE

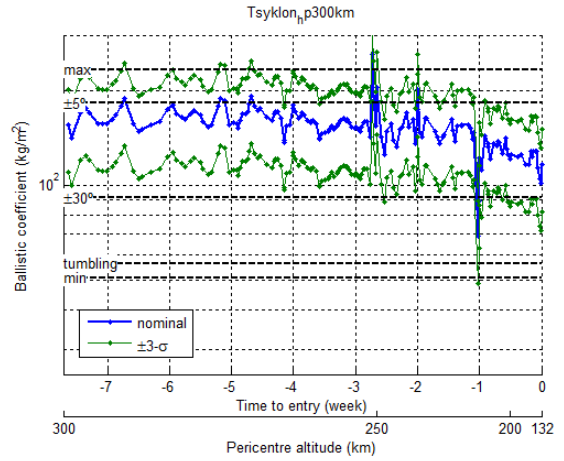


Figure 12 BC estimation, Tsyklon second stage, altitude below 300 km

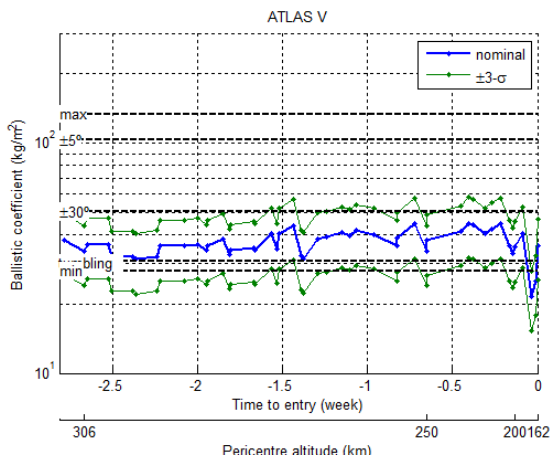


Figure 13 BC estimation, Atlas V second stage, altitude below 300 km

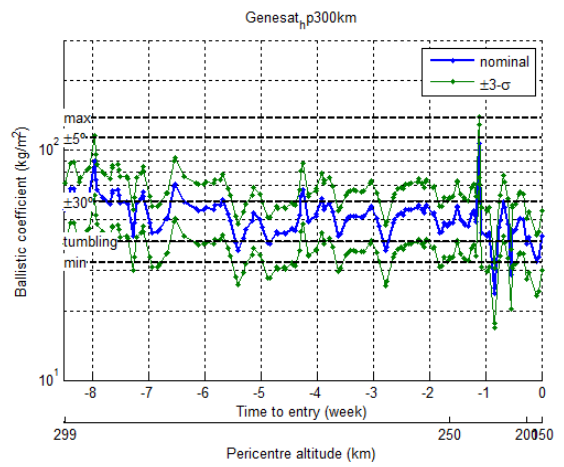


Figure 14 BC estimation, GeneSat-1 second stage, altitude below 300 km

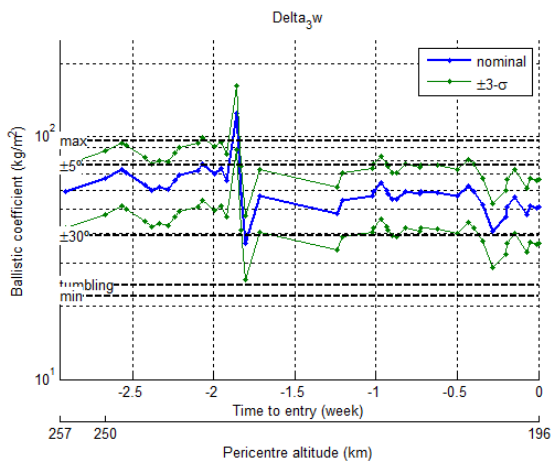


Figure 15 BC estimation, Delta second stage, altitude below 250 km

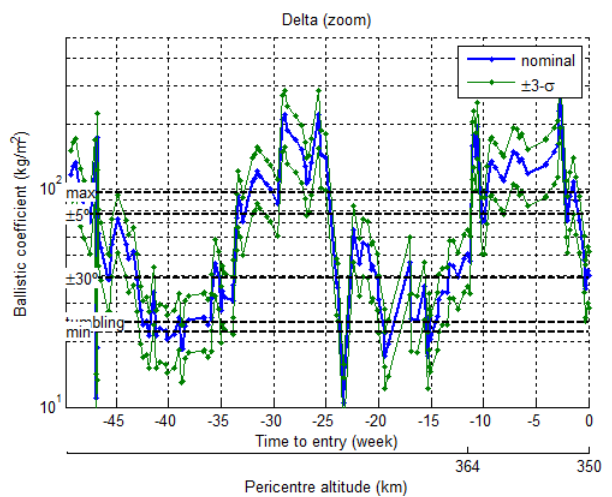


Figure 16 BC estimation, Delta second stage, altitude around 350 km

For altitudes above 250-300 km, a periodicity in the BC profile (10-15 weeks period) is encountered in Tsyklon and Delta, see for example in Fig. 16. These two cases differ from the others for an initial eccentricity of the orbit: this feature combined with the movement of the argument of the pericentre could explain the periodicity. However, a careful investigation of BC correlations with the orbital parameters and an analysis of all the attitude perturbations should be done to better characterize this variability. Also, it is noted that BC variability is slightly wider than the min-max expected BC: this could be related to the model uncertainties in both atmosphere and aerodynamics.

## 5 CONCLUSIONS

The main results of the study of the re-entry of rigid bodies that present commonalities with GOCE from an aerodynamic point of view have been shown in this work.

The space objects selection process has been based on the analysis of the aerodynamics and flying qualities for simple shapes as short and elongated cylinders and boxes. They are considered well representative respectively of rocket bodies (upper stages) and payloads (cubeSats). Based on the DISCOS database, 17 space objects have been identified (matching the list of criteria identified) and among them 5 objects have been selected for further analysis.

Globally it is concluded that elongated bodies that can be approximated as simple cylinder and boxes, potentially show stable attitude behaviour during their decay below altitude of 250 km. For such objects, knowing the **attitude behaviour significantly reduces the variability in the ballistic coefficient and therefore allows a better estimation of the re-entry time**. The attitude performance models extracted from the TLE analysis results aligned with the expected behaviour; however, the approach followed should be extended to a larger number of objects to properly verify its applicability.

A generalization of the aerodynamic stability analysis for different object shapes is not straightforward and requires dedicated analysis. However, the extraction of an attitude performance model from the analysis of the TLE remains a potentially valid approach.

## 6 REFERENCES

1. Saundres A., Swinerd G. & Lewis H (2009). *Preliminary results to support evidence of thermospheric contraction*. Advanced Maui Optical and Space Surveillance Technologies Conference.
2. Santoni F., Cordelli E., & Piergentili F. (2013). *Determination of Disposed-Upper-Stage Attitude Motion by Ground-Based Optical Observations*.

Journal of Spacecraft and Rockets, Vol. 50, No. 3.

3. Bonetti D., Parigini C., De Zaiacomo G., Pontijas Fuentes I., Blanco Arnao G., Riley D., & Sánchez Nogales M. (2016). *PETBOX: FLIGHT QUALIFIED TOOLS FOR ATMOSPHERIC FLIGHT*, 6th International Conference on Astrodynamics Tools and Techniques (ICATT), Darmstadt, Germany.
4. Haya-Ramos, R., Peñín, L. F., Parigini, C., & Kerr, M. (2011). *Flying Qualities Analysis for Re-entry Vehicles: Methodology and Application*. Presented at AIAA GNC/AFM/MST 2011 Conference, Portland, Oregon.
5. <https://discosweb.esoc.esa.int/web/guest/home;jsessionid=92e1325f72d5b296f03974862697>, retrieved on March 2017.